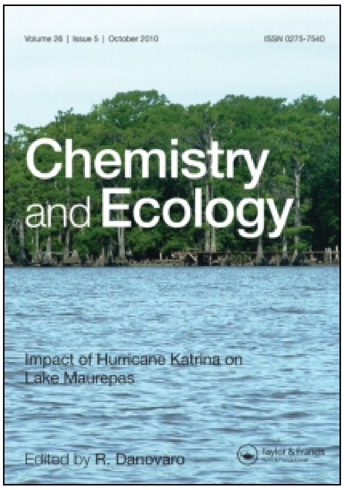

Chemistry and Ecology
Publication details, including instructions for authors and subscription information:
http://www.informaworld.com/smpp/title~content=t713455114

Inertial oscillations and particle flux interactions in a marine protected area in Gulf of Naples

L. Roselli[a]; C. Manno[b]; G. Spezie[a]
[a] Department of Enviromental Sciences, University of Napoli Parthenope, Napoli, Italy [b] Department of Biology Oceanography, The National Institute of Oceanographic and Applied Geophysics (OGS), Sgonico, (TS), Italy

To cite this Article Roselli, L. , Manno, C. and Spezie, G.(2007) 'Inertial oscillations and particle flux interactions in a marine protected area in Gulf of Naples', Chemistry and Ecology, 23: 2, 177 — 190
To link to this Article: DOI: 10.1080/02757540701197937
URL: http://dx.doi.org/10.1080/02757540701197937

Chemistry and Ecology
Vol. 23, No. 2, April 2007, 177–190

Taylor & Francis
Taylor & Francis Group

Inertial oscillations and particle flux interactions in a marine protected area in Gulf of Naples

L. ROSELLI*†, C. MANNO‡ and G. SPEZIE†

†Department of Enviromental Sciences, University of Napoli Parthenope, Via De Gasperi, 5 80133-Napoli, Italy
‡The National Institute of Oceanographic and Applied Geophysics (OGS) Department of Biology Oceanography, Borgo Grotta Gigante 42/C 34010-Sgonico (TS), Italy

(Received 30 May 2005; in final form 7 December 2006)

The area between the island of Capri and Punta Campanella was investigated from June to November 2003. Punta Campanella separates the Gulf of Naples from the Gulf of Salerno and has been declared a marine protected area in 1997. The study area has a particular interesting topography, due to the presence of a sill situated at a depth of 80 m. Samples were collected by instruments carried on a mooring array (sediment trap, current meters, and temperature sensors) and by CTD cast (along transects perpendicular to the coast). We observed most important fluctuations in the temperature spectra (corresponding to the inertial oscillations period), in August. The total mass flux was 585.67 mg m^{-2} d^{-1} in the summer, while in early autumn the flux exhibited values one order of magnitude higher than in summer (1539.97 mg m^{-2} d^{-1}). The main focus of this study was to understand the influence of the internal waves on the particle flux. During the autumn, in the particle flux collected, there is a strong resuspension component, and the observation that the enhanced inertial oscillations and increased sedimentation occur at the same time allows us to presume that the inertial oscillations could be one of the reasons for the resuspension process during the sampling period.

Keywords: Gulf of Naples; Inertial oscillations; Particle fluxes

1. Introduction

The Gulf of Naples is located over the continental shelf in the south-eastern part of the Tyrrhenian Sea (Western Mediterranean), with an average depth of 170 m over and an area of about 870 km^2. Due to its peculiar morphology, it represents a prototype of an almost rectangular semi-enclosed sea, and so it is very interesting for oceanographic purposes. In this area, two subsystems coexist: a eutrophic coastal zone and an oligotrophic area [1]; the location and width of the boundary between the two subsystem are variable over the seasons [2, 3]. The phytoplankton population is dominated by diatoms and phytoflagellates for most of year [4]. The annual cycle of the autotrophic biomass is characterized by an initial growth phase

*Corresponding author. Email: lea.roselli@fg.ismar.cnr.it

Chemistry and Ecology
ISSN 0275-7540 print/ISSN 1029-0370 online
http://www.tandf.co.uk/journals
DOI: 10.1080/02757540701197937

in winter, a second growth phase in late spring–summer, and a third growth phase in the autumn [5].

Ribera d'Alcalà *et al.* [5] observed a regularity in the occurrence of species against the quantitative interannual variability and suggested that biological rhythms regulate the temporal dynamics of the communities, whereas the abiotic forcing modulates the amplitude of the growth phases. In the gulf, three main masses water can be found, depending on the dynamic seasonal situation. The first has its origin in the Atlantic Ocean, Atlantic Water (AW), and the latter is Levantine Intermediate Water (LIW), with hydrological characteristics within the gulf of $T = 14.2\,°\mathrm{C}$, $S = 38.65$, and $\sigma_t = 29.0$; the last is Tyrrhenian Surface Water (TSW) [1, 6].

The circulation is generally characterized by a low-frequency dynamic (period >24 h), influenced by the meteorological conditions of the Tyrrhenian Sea; and a high-frequency dynamic (period <24 h), dominated by inertial oscillations. The inertial oscillations are caused by abrupt variations of the current direction or by changes in the winds field, and they have a period of about 17–18 h [7]. The understanding of the dynamics in this gulf is particularly interesting due to the fact that the littoral area is heavily influenced by the land runoff from a very densely populated region.

The headland of Punta Campanella (belonging to the Sorrentina Peninsula) separates the Gulf of Naples from the Gulf of Salerno and has been declared a marine protected area in 1997. In the past 20 yr, this area suffered environmental damage due to the use of trawl nets, explosives, urban and industrial waste waters, and poachers of date mussels [8]. The Sorrentina Peninsula is characterized by high calcareous cliffs that decline in the sea at depths of more than 50 m, and it is separated from the Island of Capri from the Bocca Piccola Area. Bocca Piccola has a particularly interesting topography due to the presence of a sill situated at a depth of 80 m, which slopes rapidly down as far as the 1000-m isobath. In this area, the occurrence, during the summer, temperature oscillations corresponding to the thermocline stratification may be due to the presence of internal waves. These waves may cause vertical motion, influencing current velocity along the vertical component. Convincing evidence is emerging that internal solitary waves and other long wave packets propagating in shallow seas can frequently stimulate remarkably elevated rates of resuspension of sedimentary material [9].

Several authors have described the physical phenomenon of internal waves [10–20]. Motions at near-inertial and tidal frequencies are spread into the basin interior by propagating internal waves that may break in certain areas, thereby causing mixing [21]. Particular topographic sites may be important for internal wave breaking and thus localized enhanced mixing [22–24]. The presence of sills causes stronger currents that release large amounts of turbulent kinetic energy, which has a tremendous impact on the physical and biological components [25].

The aim of this study was to characterize inertial oscillations and to evaluate the role of internal waves in resuspending sediment from the bottom boundary.

2. Materials and methods

This study included two time series of data collected from the 9 June to 11 September and from 11 September to 10 November 2003 using a sediment trap and oceanographic instruments (current meter and temperature sensors), carried on bottom-tethered mooring deployed at 40° 34′ 538″ N, 14° 18′ 831″ E in the area of Punta Campanella (figure 1). The oceanographic cruise was conducted aboard the N/O *Universitatis*. In addition, hydrological sampling by CTD was carried out along transects perpendicular to the coast.

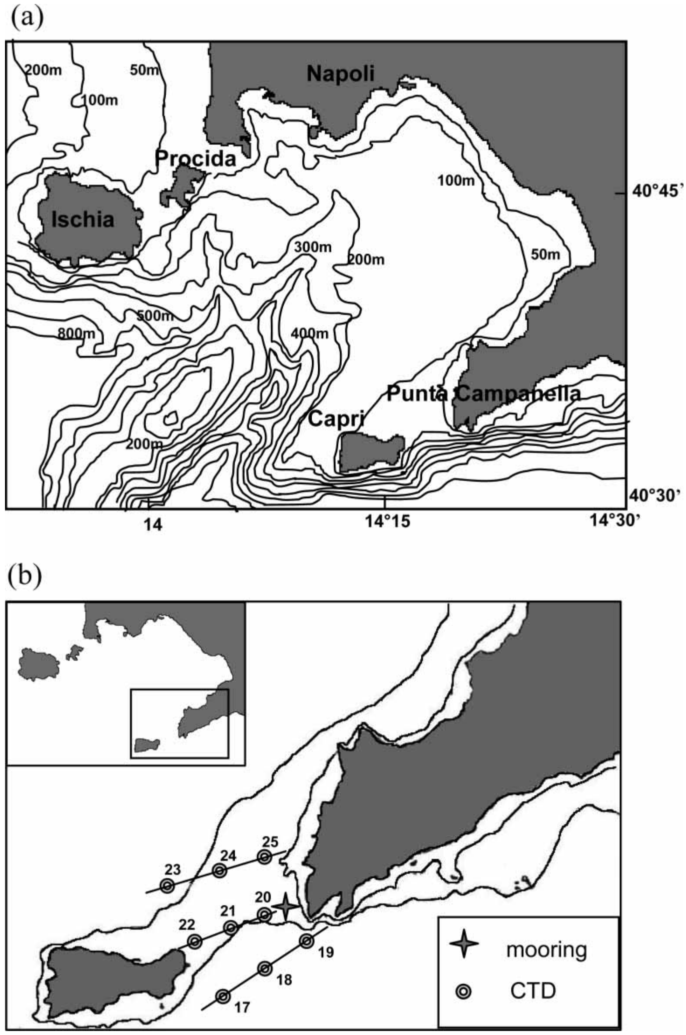

Figure 1. (a) Gulf of Naples and (b) mooring site and CTD stations in the Punta Campanella area.

2.1 *CTD profiles*

Hydrological casts were carried out using an SBE 9/11 Plus CTD, with temperature and conductivity sensors, on 10 June and 11 November 2003. During the cruises, the CTD temperature was controlled by means of two SIS RTM 4200 digital reversing platinum thermometers. At every station, several replicate samples were collected at all depths and analysed on board by means of an Autosal Guidline Salinometer. CTD profiles were collected along three perpendicular transects to the coast, close to the mooring station. On 10 June, from stations No. 17 to No. 19, salinity and density data were not available because the conductivity sensor did not work.

2.2 *Currents and temperature data*

Currents were monitored with Aanderaa RCM7 current meters, at depths of 25 and 65 m, and the frequency of acquisition was set at 30 min. Temperature was detected using a Sea-Bird

Electronics temperature sensor at depths of 30 m, 38 m, 46 m, and 52 m, and the frequency of acquisition was set at 10 min. Data were filtered with band-pass filtering (filter degree 3), to attenuate the high-frequency signal due to diurnal and semidiurnal tidal oscillations and to characterize inertial oscillations.

To calculate the eddy kinetic energy (EKE), the following equation was used: EKE $= (1/2)[(u')^2 + (v')^2]$. In addition, wind data were obtained from the Meteorological Station of S. Agata (Sorrentina Peninsula). Current data at 25 m of depth were not available from 11 September to 10 November because the current meter did not work.

2.3 *Sediment trap sampling and analyses*

Sediment traps were deployed at a depth of 76 m (9 June–11 September; Trap BP1) and 68 m (11 September–10 November; Trap BP2). Each sediment trap (Hydro-Bios Multi Sediment Trap MST 24) carried only one receiving cup with a collecting area of 0.01515 m^2 and was fitted with a plastic baffle mounted in the opening, to prevent large organisms entering. In the receiving cup, a 5% buffered formalin-sea water solution was used as a preservative. Upon recovery, samples were kept refrigerated (~2–4 °C) in the dark until analysis. Each sample was then precisely divided, for subsequent analysis, into a series of replicate fractions (or subsamples), according to Heussner *et al.* [26]. Prior to splitting, swimmers (zooplanktonic organisms that can enter the receiving cups while alive) were removed because they can introduce an erroneous active component in the measurement of the passive flux [27]. Then, the original sample was diluted in a suitable volume of 0.4 μm of filtered sea water and kept homogenized with an orbital stirrer; while stirring, small equal volumes of the suspension were successively poured into several beakers using a high-precision peristaltic pump. Replicate fractions were vacuum-filtered through pre-weighed 0.45-μm Millipore filters for total mass determination and through pre-weighed 0.45-μm Whatman GF/F filters for organic carbon (OC) analyses. Filters were then desalted by briefly washing with distilled water, dried at 60 °C, and weighed. OC was measured by combustion in an elemental analyser (LECO CS 125); filters were previously treated with 2 N H_3PO_4 and 1 N HCl (UNESCO, 1994). Faecal pellets were counted, under a dissection microscope, in the whole sample or some replicate fractions and converted to fluxes (no. pellets m^{-2} d^{-1}) by dividing the total number by the time interval and the trap collection area.

3. Results

3.1 *Vertical sections*

The results focus on three transects; each transect includes three CTD stations. CTD casts were collected on 10 June 2003, during the summer survey, and on 11 November 2003, during the autumnal survey. Potential temperature, salinity, and density data are shown in figure 2. In the summer (figure 2a), surface waters were characterized by temperature $T = 24$ °C, salinity $S = 38.64$, and density $\delta = 26.34$ kg m^{-3}. The thermocline isotherms were found between 10 and 40 m, followed by a continuous mixed layer almost to the bottom. In the autumn (figure 2b), the surface mixed layer was 50 m thick with values of $T = 20$ °C, $S = 37.90$, and $\delta = 27.00$ kg m^{-3}. The thermocline layer was found at depths of 55–70 m, and below this layer, a mixed layer was present. We observed, in the both periods, Tyrrhenian Surface Water (TSW; $T = 21$ °C; $S = 37.80$; $\delta = 26.60$ kg m^{-3}) in the surface layer, and Levantine Intermediate

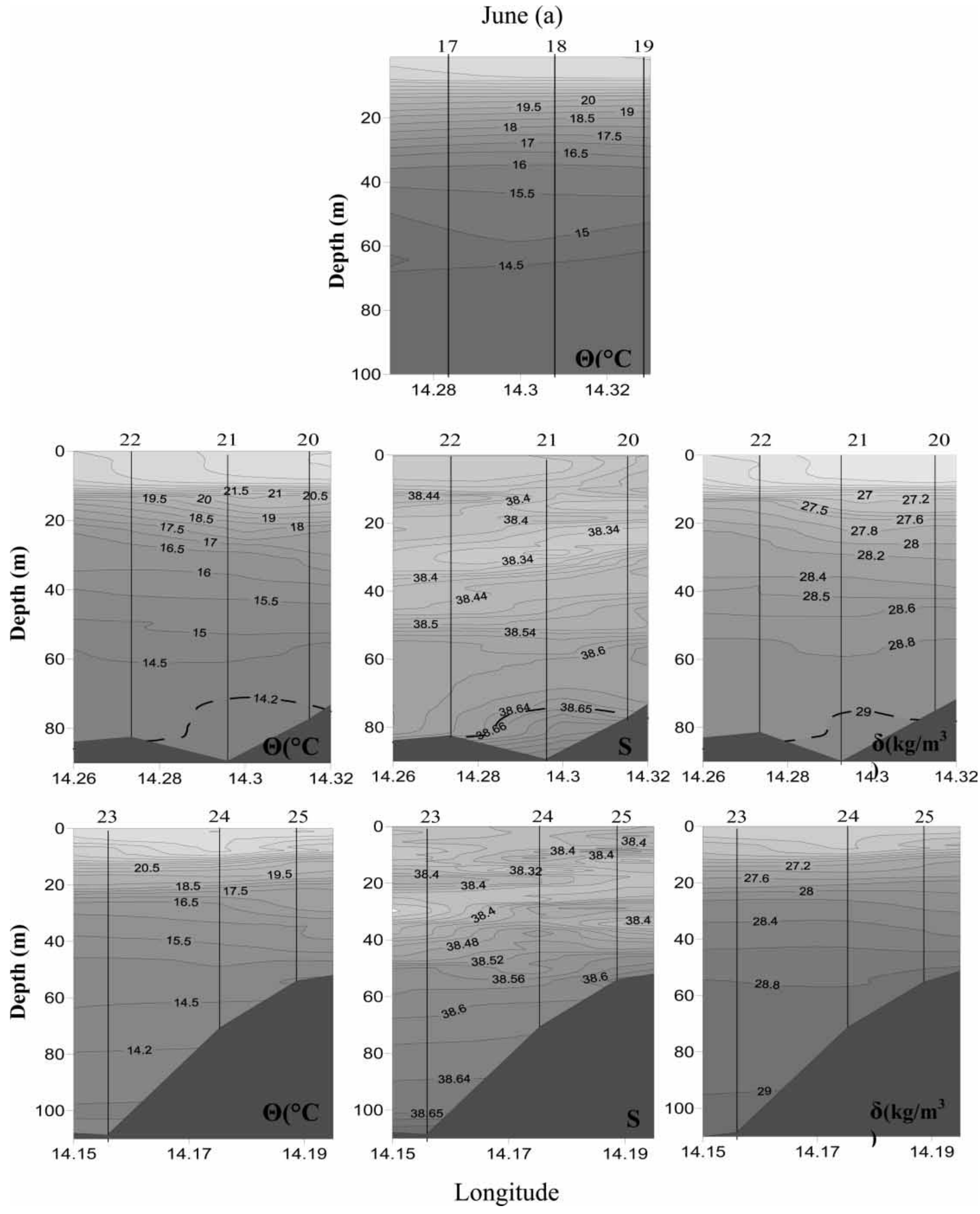

Figure 2. Vertical sections of potential temperature (°C), salinity and density (kg m^{-3}) in (a) June and (b) November along the transects.

Water (LIW; $T = 14.2\,°\mathrm{C}$, $S = 38.65$, $\delta = 29.0\,\mathrm{kg\,m^{-3}}$) flowing in the gulf across the sill at a depth of 80 m.

3.2 *Temperature and velocity spectra*

The spectra of the temperature and velocity fluctuations show the strongest peaks at the 7–8-d frequency periods, followed by diurnal and semidiurnal frequencies, and also in the 17- and 18-h overtones that represented the inertial oscillation period and are not evident in each

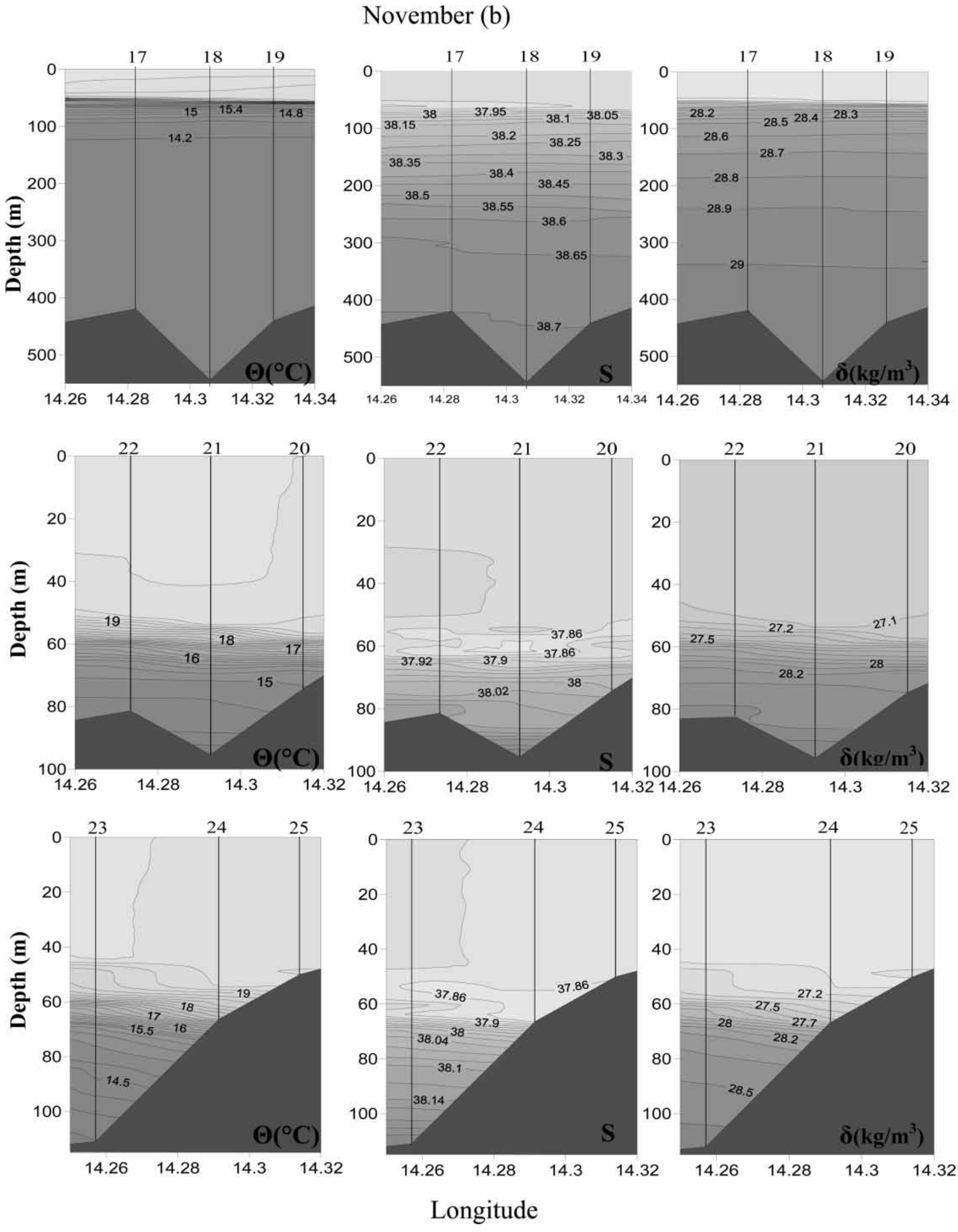

Figure 2. Continued.

spectrum. Velocity vector is divided into two components, u along the E–W direction and v along the N–S direction. In August, temperature spectra show higher peaks diminishing with depth; in September, they show the largest peaks in the middle sampling levels, and in October, no particular peak is present. The spectra of the velocity u and v component show the strongest peaks in August, September, and October. The relatively large amplitude of the u component velocity variations then highlights the predominantly east–west zonal flows.

3.3 *Time series of temperature, currents, and wind*

Direct temperature, currents, and wind observations are used to describe the properties of internal waves. The time series (9 June–31 October) of temperatures collected at the mooring (figure 3) exhibited wider fluctuations in three different times, with stronger oscillations into the surface layer. The first significant inertial oscillation (30 July–5 August) is a result of strong wind variation coming from the northwest to the south-east and a rapid variation in the current direction, especially at a depth of 25 m. The second inertial oscillation (15 September–21 September) is due to the inversion of the current from SE to NW, and the period of fluctuations is around 5–6 d. In both cases, the temperature fluctuations spread into the thermocline, behaving as a waveguide. The last obvious signal of inertial oscillation (17–23 October) is found at deeper levels, near the bottom, following a strong south-eastward current (figure 4).

Table 1 shows the ranges of wind and current intensity and the temperature fluctuations in the water column during the inertial oscillations events. The current at 65-m depth exhibits high-intensity variations during three events: from 30 July to 5 August, the range is 1.5–6.5 cm s^{-1}; in the week 15–21 September, the range is 1.5–1.8 cm s^{-1}; and from 17 to 23 October, the range is 1.5–15.3 cm s^{-1}. The wider temperature oscillations correspond to the current variations: these can be observed in relation to the surface layer, at 25-m depth (17.5–26.3 °C), during the first event. From 15 to 21 September, the ranges vary from about 5 to 6° to a depth of 46 m. In the last period, the fluctuations are very noticeable near the bottom, at depths of 46 m, 52 m, and 65 m, with ranges fluctuating from about 4 to 5°.

3.4 *Sinking particle: qualitative observations*

The BP1 sediment trap collected negligible amounts of swimmers, while the BP2 trap included large amounts of zooplanktonic organisms. In both traps, the more abundant organisms were represented by copepods, pteropods, and polychaetes. During the autumn, the trap included a strong benthonic component, as polychaetes, pecten, calcareous algae, and copepods were represented principally by exuvie.

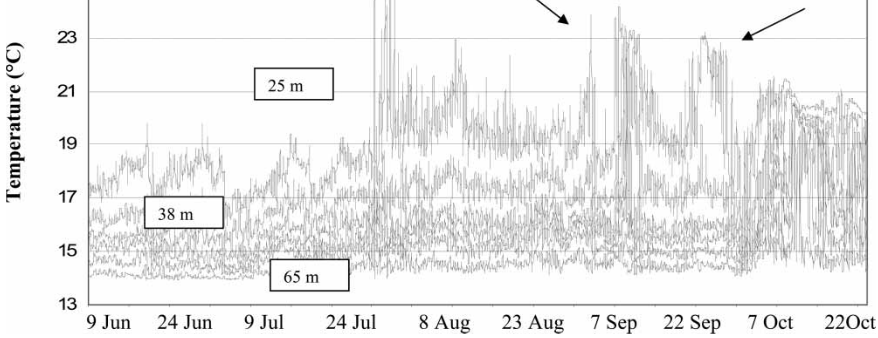

Figure 3. Time series of temperature (°C) at depths of 25, 30, 38, 46, 52, and 65 m.

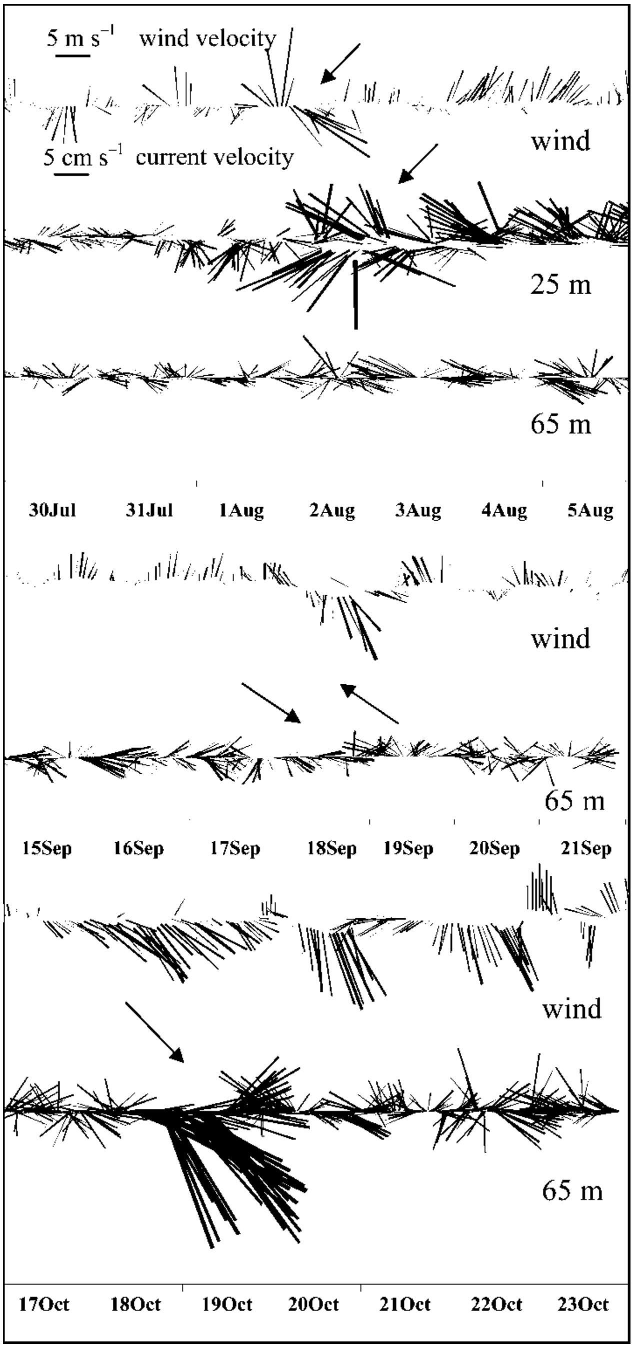

Figure 4. Stick plots (cm s^{-1}) of the wind (m s^{-1}) and of the currents (cm s^{-1}) at 25 and 65 m depth.

The dominant morphological types of faeces showed a cylindrical shape. In the summer period, pellets were the best preserved. In the autumn, pellet samples were more degraded than in the summer samples; they were fragmented lengthwise (with the peritrophic membrane disrupted at many points) and less densely packed. The pellets observed in BP2 were generally

Table 1. Range of the wind and current intensity and temperature fluctuations in the water column during the inertial oscillations events.

Day	Wind ($m\,s^{-1}$)	25 m current ($cm\,s^{-1}$)	65 m current ($cm\,s^{-1}$)
30 Jul–5 Aug	0.1–6.7	1.5–11.7	1.5–6.5
15 Sep–21 Sep	0.0–3.2	–	1.5–5.8
17 Oct–23 Oct	0.1–8.0	–	1.5–15.3

Day	Temperature (°C)					
	25 m	30 m	38 m	46 m	52 m	65 m
30 Jul–5 Aug	17.5–26.3	15.8–18.8	15.3–17.4	14.5–16.6	14.3–16.3	14.3–15.7
15 Sep–21 Sep	18.7–24.1	16.1–22.8	15.3–22.7	14.8–22.5	14.5–16.2	14.1–15.3
17 Oct–23 Oct	20.0–21.4	18.8–21.1	17.0–20.6	16.2–20.6	14.8–20.4	14.3–19.5

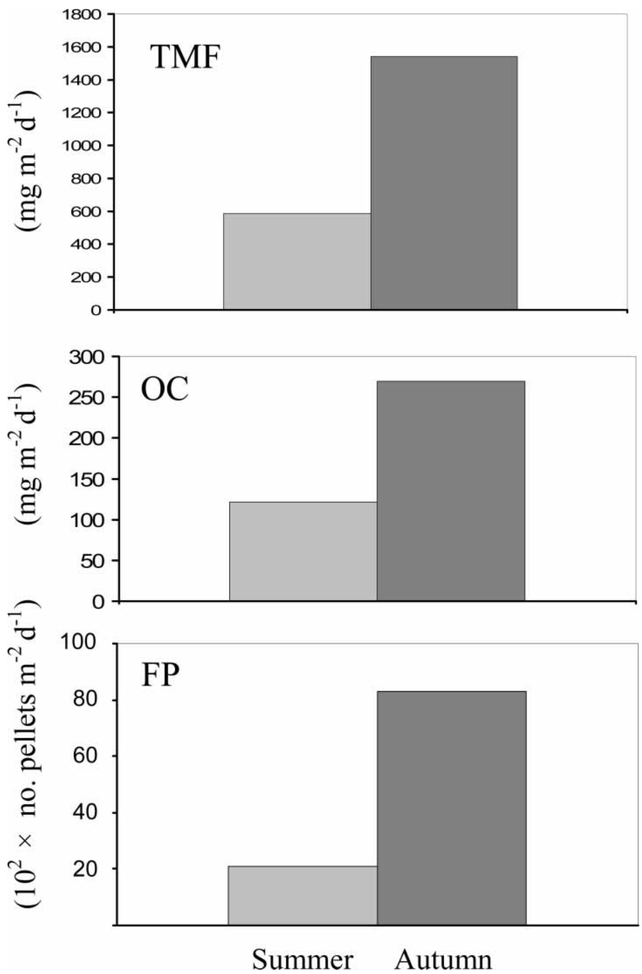

Figure 5. Total mass flux (TMF, $mg\,m^{-2}\,d^{-1}$), organic carbon flux (OC, $mg\,m^{-2}\,d^{-1}$) and faecal pellets flux (FP, no. pellets $m^{-2}\,d^{-1}$) as measured by summer (BP1) and autumn (BP2) trap.

darker in colour than the pellets collected in BP1. In both samples, the pellet sizes were in two principal classes: 500–700 μm and 160–300 μm.

3.5 *Sinking particle: quantitative observations*

During the summer (June–September), the total mass flux was 585.67 mg m^{-2} d^{-1}, while in the early autumn (September–November) the flux exhibited values are order of magnitude (1539.97 mg m^{-2} d^{-1}) higher than in summer (figure 5a).

The OC was 121.6 mg m^{-2} d^{-1} during the first period and 269.8 mg m^{-2} d^{-1} during the second period, contributing to 21 and 18% of the total mass flux (figure 5b). Faecal pellets (FP), despite showing the same order of magnitude in both traps, exhibited a higher flux in BP2 (8.30×10^4 pellets m^{-2} d^{-1}) than in BP1 (2.11×10^4 pellets m^{-2} d^{-1}) (figure 5c).

4. Discussion

The hydrodynamic structure in the Gulf of Naples has been described by several authors [6, 28, 29]. The Gulf of Naples is sometimes strongly influenced by the presence of near-inertial oscillations which tend to vanish or grow in different points of the gulf. At the latitude of the Gulf of Naples, the Coriolis frequency corresponds to a period of about 17 h, and inertial phenomena are observed to prevail during the summer and autumn when the thermocline is well developed in the Tyrrhenian Sea, as deduced from hydrological profiles from various oceanographic surveys carried out in 1977–1981 [7]. Results obtained in this study bear out, after 20 yr, the persistence of inertial oscillations in the Bocca Piccola.

Typically, inertial oscillations depend on a rapid variation in the current direction caused by a sudden change in the wind field. The origin of internal waves in the Bocca Piccola is attributed primarily to the topography of the sill: the current flowing over the sill generate internal waves because of the abrupt bottom variation the passage of these waves produces vertical mixing. During summer 2003, we observed a single significant inertial event (from 30 July to 5 August) as a result of a variation in the direction and intensity of the current, due to the wind.

In early autumn, inertial events are more intense than in the summer. The first event, during the second week of September, follows current inversion. Between 17 and 23 October, the inertial oscillatory current is stronger than the others, and the flux is observed on the sill from the north-west to the south-east. This study suggests that the inertial oscillation events are correlated with the wind at periods representing the passage of atmospheric fronts.

Table 2 shows the EKE values of currents as a weekly average. According to Filonov *et al.* [18], the existence of a sill in the presence of high kinetic energy is an appropriate condition for the generation of internal waves. EKE exhibits a strong increase in the upper and bottom layers corresponding to inertial oscillation as a result of strong current fluctuations. During the summer, the energy values are found to be high also in the week following the inertial event and decrease rapidly thereafter; therefore, in September and October, higher EKE values are observed during inertial oscillations periods.

The weak dependance from depth of the seasonal changes in eddy energy implies that the relative importance of wind-generated eddy energy is maximal at a depth where the general (baroclinic) variability level is low. Accordingly, a significant correlation is found between the seasonal cycle in the variance of wind stress and the seasonal cycle in eddy energy [30]

Figure 6 shows the vertical temperature profiles during the whole sampling period and underlines the stronger and deeper stratification of the water column (from surface to 50-m

Table 2. Eddy kinetic energy (EKE, cm^2 s^{-2}) calculated on previous, corresponding (shown in bold) and subsequent week to the inertial oscillations.

Depth (m)	Day	EKE (cm^{-2} s^{-2})
25	23 Jul–29 Jul	5.99
	30 Jul–5 Aug	**10.92**
	6 Aug–12 Aug	11.19
	13 Aug–19 Aug	4.11
65	23 Jul–29 Jul	1.81
	30 Jul–5 Aug	**3.27**
	6 Aug–12 Aug	3.15
	13 Aug–19 Aug	1.37
	8 Sep–14 Sep	2.31
	15 Sep–21 Sep	**3.01**
	22 Sep–28 Sep	2.07
	10 Oct–16 Oct	4.55
	17 Oct–23 Oct	**8.62**
	24 Oct–31 Oct	3.88

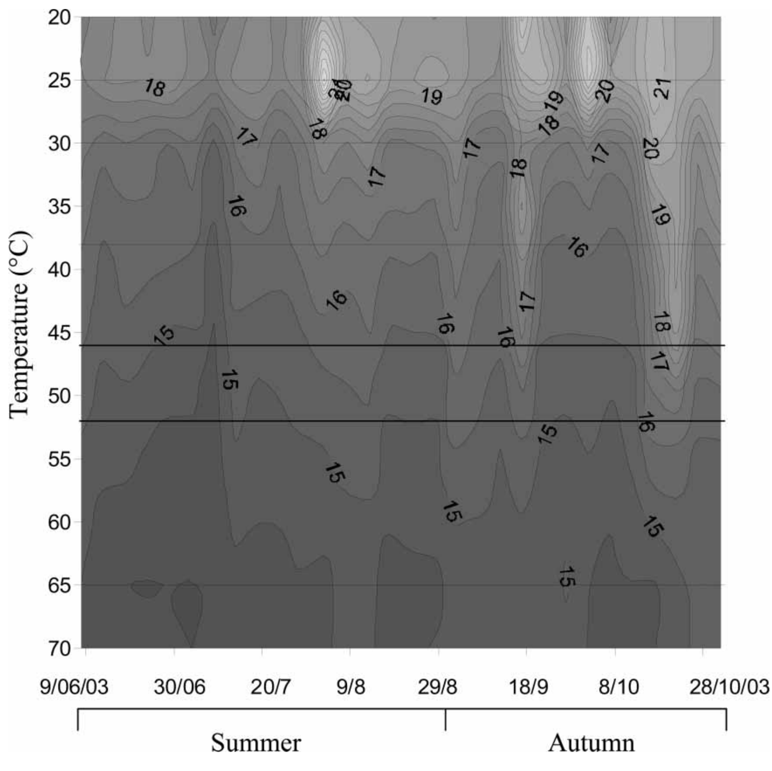

Figure 6. Vertical sections of potential temperature (°C) from June to October.

depth) during autumn. We found that inertial oscillations propagate in the deeper sampling levels in early autumn and for a longer time (figure 3); this could be due to the stratified surface layer that could hinder vertical energy propagation.

These results are in agreement with De Maio [7], who showed that even though the energetic input relative to inertial events is associated with passing storm systems, the water stratification is the main condition necessary for the existence of these current oscillations because in winter (when storms are stronger and more numerous), not so many inertial events are observed as during the summer.

Despite the presence of a well-stratificated thermocline that could obstruct downward particulate fluxes in the water column, during autumn the flux exhibits values one order of magnitude higher than in the summer. Unfortunately, there are no references on the particle flux in the Gulf of Naples. However, several authors have observed in other areas of the Mediterranean Sea maximum peak fluxes during the summer months ranging from 0.4 to 2.0 g m^{-2} d^{-1}, and fluxes between 0.1 and 0.6 g m^{-2} d^{-1} [30–35] during the autumn. In our samples, the total mass flux from September to November was 1.5 g m^{-2} d^{-1}, the highest ever reported for the autumn with respect to the other Mediterranean values.

Cacchione *et al.* [36] observed that if high-frequency internal waves shoal and break along the seafloor in the seasonal pycnocline, erosion and resuspension of bottom sediment might occur. In this study, we found evidence of resuspension of the sediment collected in the autumn:

(1) Faecal products are darker in colour, and according to Heussner *et al.* [26], the darker faecal products have a benthonic origin. Besides, in this period, pellets were fragmented and less densely packed (as a consequence of a long exposure to degradation mechanisms), suggesting contact with the sediment.
(2) The presence of a strong benthonic component such as polychaetes and calcareous algae has been found.

The observation that the enhanced inertial oscillations and increased sedimentation occur at the same time, when resuspension of the sediment was observed, allows us to presume that the inertial oscillations could be one of the causes contributing to the resuspension process.

However, this study was carried out near the coast where currents are strong and variable, and it is possible than in the autumn, the sediment resuspension is due to turbulent mixing by wind or by breaking of surface waves.

One previous study in the Thermaikos Gulf in Aegean Sea [37] showed that sampling periods were characterized by stronger near-bed currents, while relatively weak internal wave motions dominated the periods of stratification. The near-bed currents showed strong coherence with the wind during the period of full homogenization, whereas during stratification periods, the wind provided indirect forcing evident mostly in the internal-wave bands. The site was too deep (63 m) for the surface waves to cause any sediment resuspension. In conclusion, the observed near-bed currents at the site of interest did not appear to produce significant local resuspension of sediment; notably, the current–turbidity correlation suggested a shoreward transport of suspended material.

This work is only a preliminary study because, currently, our results are not sufficient to prove the relationship between internal waves and sediment resuspension in this area. In the future, to understand the internal wave effects on sediment resuspension, it would be very useful to collect particles by time-series sediment traps deployed from the surface to the bottom. Moreover, it could be very interesting to understand the internal wave effects on biological production in the surface layers through a synoptic campaign of measurement that synchronizes sampling with inertial oscillations events, also considering the various biological parameters (chlorophyll, phytoplankton, and nutrient), that would be specific indicators of vertical advection from deeper layers.

Acknowledgements

We are grateful to G. Scherillo, V. Soricillo, and L. Rovito (Università degli Studi Napoli ‘Parthenope’), for putting the laboratory at our disposal, and to S. Tucci (Dipteris, Università degli Studi di Genova), for his generosity in lending us the sediment traps. Thanks are due to D. Flocco (University of Cambridge), for useful advice on the 'English form' in this paper. We gratefully acknowledge the crew of the *Universitatis*, for the deployment/recovery of the mooring, particularly Dr. P. Siena.

References

[1] G.C. Carrada, T.S. Hopkins, G. Bonaduce, A. Ianora, D. Marino, M. Modigh, d'Alcalà M. Ribera and B. Scotto di Carlo. Variabilità in the hydrographic and biological features of the Gulf of Naples. P.S.Z.N.I. *Mar. Ecol.*, **1**, 105–120 (1980).

[2] G.C. Carrada, D. Marino, M. Modigh, d'Alcalà M. Ribera. Variazioni spaziali in acque superficiali di nutrienti, clorofilla ed associazioni fitoplanctoniche nel Golfo di Napoli. In *Quaderni del Laboratorio di Tecnologia della Pesca* (1981).

[3] D. Marino, M. Modigh and A. Zingone. General features of phytoplankton communities and primary production in the Gulf of Naples and adjacent waters. In *Marine Phytoplankton and Productivity*, Holm-Hansen O., Bolis L. and Gilles R. (Eds), pp. 89–100, Springer, Berlin (1984).

[4] B. Scotto di Carlo, C.R. Tomas, A. Ianora, D. Marino, M.G. Mazzocchi, M. Modigh, M. Montresor, L. Petrillo, d'Alcalà M. Ribera, V. Saggiomo, A. Zingone Uno studio integrato dell'ecosistema pelagico costiero del Golfo di Napoli. *Nova Thalassia*, **7**, 99–128 (1985).

[5] d'Alcalà M. Ribera, F. Conversano, F. Corato, P. Licandro, O. Mangoni, D. Marino, M.G. Mazzocchi, M. Modigh, M. Montresor, M. Nardella, V. Saggiomo, D. Sarno, A. Zingone. Seasonal patterns in plankton communities in a pluriannual time series at a coastal Mediterranean site (Gulf of Naples): an attempt to discern recurrences and trends. *Cienc. Mar.*, **67**(Suppl. 3) (2004).

[6] A. De Maio, M. Moretti, E. Sansone, G. Spezie, M. Vultaggio. Dinamica delle acque del Golfo di Napoli. Diffusione delle acque dolci che pervengono nel Golfo (aprile, settembre, ottobre 1977). *Annali I.U.N.*, **47–48**, 201–213 (1978–1979).

[7] A. De Maio, M. Moretti, E. Sansone, G. Spezie, M. Vultaggio Outline of Marine Currents in the Bay of Naples and Some Considerations on Pollutant Transport. *Il Nuovo Cimento*, **8C**, 955–969 (1985).

[8] F. Cicogna, G.F. Russo. Il Parco Marino di Punta Campanella: una lunga storia, ora realtà. *Uomo e Natura*, **8**,10–15 (1998).

[9] D. Bogucki, T.D. Dickey and L.G. Redekopp. Sediment resuspension and mixing by resonantly generated internal solitary waves. *J. Phys. Oceanogr.*, **27**, 1181–1196 (1997).

[10] P.G. Baines. On internal tide generation models. *Deep Sea Res. A*, **29**, 307–338 (1982).

[11] P.D. Graig. Solution for internal tide generation over coastal topography. *J. Mar. Res.*, **45**, 83–105 (1987).

[12] A.L. New. Internal tidal mixing in the Bay of Biscay. *Deep-Sea Res.*, **35**, 691–709 (1988).

[13] T.J. Sherwin. Analysis of an internal tide observed on the Malin Shelf, North of Ireland. *J. Phys. Oceanogr.*, **18**, 1035–1050 (1988).

[14] L.A. Ostrovsky, Yu. A. Strepanyants. Do internal solitons exist in the ocean? *Rev. Geophys.*, **27**, 293–310 (1989).

[15] A.L. New, R.D. Pingree. Evidence for internal tidal mixing near the shelf break in the Bay of Biscay. *Deep-Sea Res.*, **37**, 1783–1803 (1990).

[16] V.I. Vlasenko. Semidiurual internal tides in Massachusetts Bay. *Phys. Oceanogr.*, **6**, 9–16 (1991).

[17] K.G. Lamb. Numerical experiments of internal wave generation by strong tidal flow across a finite amplitude bank edge. *J. Geophys. Res.*, **99**, 843–864 (1994).

[18] A.E. Filonov, C.O. Monzón, I.E. Tereshchenko. On the conditions of internal wave generation along the west coast of Mexico. *Cien. Mar.*, **23**, 255–272 (1996).

[19] E.N. Pelinovsky. *Tsunami Waves Hydrodynamics*, p. 276, Academy of Science of Russia, Institute of Applied Physics, Nigni Novgorod (1996).

[20] J. Xing, A.M. Davies. A three-dimensional model of internal tides on the Malin-Hebrides shelf and shelf edge. *J. Geophys. Res.*, **103**, 27821–27847 (1998).

[21] C. Wunsch, R. Ferrari. Vertical mixing, energy and the general circulation of the oceans. *Annu. Rev. Fluid Mech.*, **36**, 281–314 (2004).

[22] M.C. Gregg, E. Kunze. Shear and strain in Santa Monica Basin. *J. Geophys. Res.*, **96**, 16709–16719 (1991).

[23] H. Van Haren, L. Maas, J.T.F. Zimmerman, H. Ridderinkhof, H. Malschaert. Strong inertial currents and marginal internal wave stability in the central North Sea. *Geophys. Res. Lett.*, **26**, 2993–2996 (1999).

[24] C. Garett. The role of secondary circulation in boundary mixing. *J. Geophys. Res.*, **95**, 3183–3189 (1990)

[25] A.E. Filonov and M.F. Lavìn. Internal tides in the Northern Gulf of California. *J. Geophys. Res.*, **108**, C5, 3151 (2003).

[26] S. Heussner, A. Monaco and S.W. Fowler, Characterization and vertical transport of setting biogenic particles in the northwestern Mediterranean. In E.T. Degens, E.I. Izdar and S. Honjo (eds) *Paritcle Flux in the Ocean*, Mitt. Geol.-Paläont. Inst., Univ. Hamburg, SCOPE/UNEP Sonderband 62: 127–147.

[27] US Global Ocean Flux Study, *US GOFS Planning Rep. No. 10* (1989).

[28] M. Moretti, E. Sansone, G. Spezie, M. Vultaggio, A. De Maio. Alcuni aspetti del movimento delle acque del Golfo di Napoli. *Annali I.U.N.*, **45–46**, 207–217 (1976–1977).

[29] A. De Maio, M. Moretti, E. Sansone, G. Spezie, M. Vultaggio. Circolazione costiera. Analisi dinamica e idrologica di una situazione osservata nel Golfo di Napoli, paper presented at the conference Unità Operative afferenti ai sottoprogetti Risorse Biologiche e Inquinamento Marino, Rome, 10–11 November 1981 (1982).
[30] S. Miserocchi, J. Faganeli, V. Balboni, S. Heussner, A. Monaco, P. Kerherve. Characteristics and sources of the settling particulate organic matter in the South Adriatic basin. *Org. Geochem.*, **30**, 411–421 (1999).
[31] D. Stammer, C. Böning, C. Dieterich. The role of variable wind forcing in generating eddy energy in the North Atlantic. *Prog. Oceanogr.*, **48**, 289–311 (2001).
[32] X. Durrieu De Madron, A. Abassi, S. Heussner, A. Monaco, J.C. Aloisi, O. Radakovitch, P. Giresse, R. Buscail. Particulate matter and organic carbon budgets for the Gulf of Lions (NW Mediterranean Sea). *Oceanol. Acta*, **23**, 6 (2000).
[33] G.F. Russo. La riserva marina di Punta Campanella: una realtà che necessita di una gestione integrata col territorio della penisola sorrentino-amalfitana, paper presented at 1st International Meeting of Mediterranean Coasts, pp. 221–226 (1995).
[34] A. Boldrin, S. Miserocchi, S. Rabitti, M.M. Turchetto, V. Baldoni, G. Socal. Particulate matter in the southern Adriatic and Ionian Sea: characterisation and downward fluxes. *J. Mar. Syst.*, **33–34**, 389–410 (2002).
[35] J. Fabres, A. Calafat, A. Sanchez-Vidal, M. Canals, S. Heussner. Composition and spatio-temporal variability of particle fluxes in the Western Alboran Gyre, Mediterranean Sea. *J. Mar. Syst.*, **33–34**, 431–456 (2002).
[36] C. Pohl, A. Löffler, U. Hennings. A sediment trap flux study for trace metals under seasonal aspects in the stratified Baltic Sea (Gotland Basin; 57j19. 20VN; 20j03. 00VE). *Mar. Chem.*, **84**, 143–160 (2004).
[37] D.A. Cacchione, L. Pratson, and A. Ogston. Internal tides, sedimentation, and seafloor slopes. *Eos*, *Trans. Am. Geophys. Union*, **80**, OS250 (1999).
[38] E. Tragou, V. Zervakis, E. Papageorgiou, S. Stavrakakis, V. Lykousis. Monitoring the physical forcing of resuspension events in the Thermaikos Gulf – NW Aegean during 2001–2003. *Cont. Shelf Res.*, **25**, 2315–2331 (2005).